

Supporting Information *for*
Facile preparation of upconversion microfibers for efficient
luminescence and distributed temperature measurement

Hanyang Li^a, Xiao Sun^a, Muhammad Khuram Shahzad^b, Lu Liu^{a*}

^aKey Laboratory of Fiber Integrated Optics Ministry, Harbin Engineering University, Harbin 150001, China.

^bNational Key Laboratory of Tunable Laser Technology, Institute of Opto-Electronics, Department of Electronic Science and Technology, Harbin Institute of Technology, Harbin 150080, China.

Address: College of science, Harbin Engineering University, 145 Nantong Street, Harbin 150001, China.

Telephone number: +86-451-8251-9850

Fax number: +86-451-8251-9850

*Email address: liulu@hrbeu.edu.cn

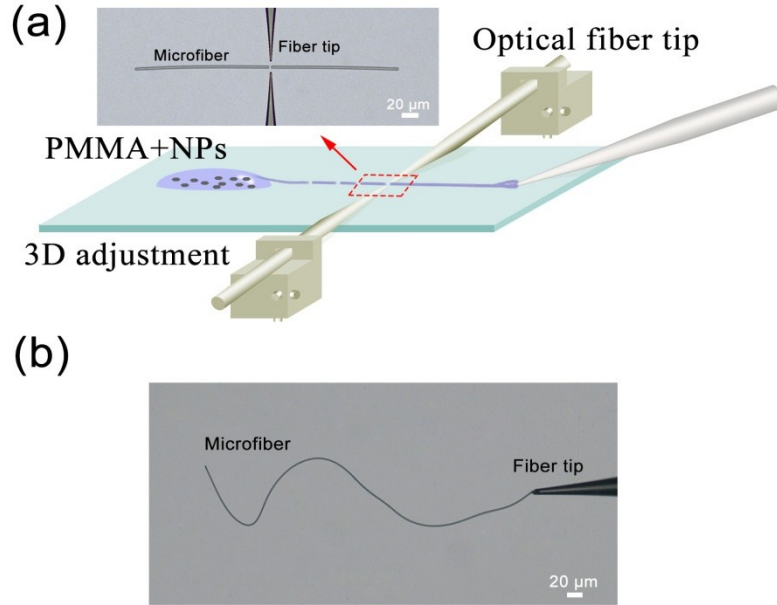


Fig. S1 (a) Schematic illustration of fabricating microfibers by direct drawing of $\text{NaYF}_4:18\% \text{Yb}^{3+}/2\% \text{Er}^{3+}/\text{PMMA}$ solution. (b) Optical microscopy image of an as-fabricated $\text{NaYF}_4:\text{Yb}^{3+}/\text{Er}^{3+}/\text{PMMA}$ microfiber.

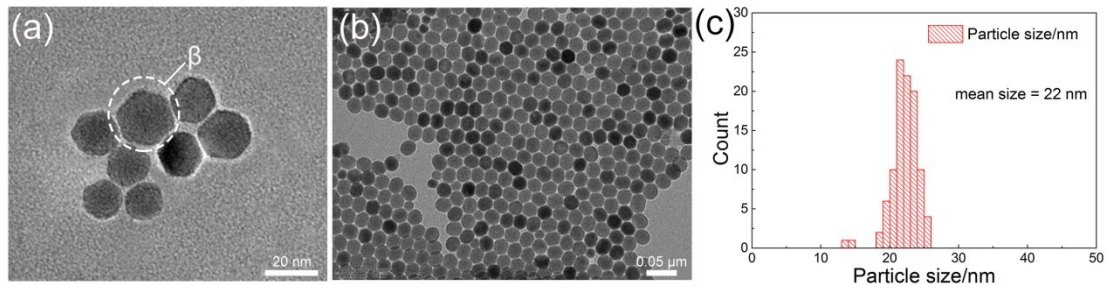


Fig. S2 (a) A typical TEM image of $\text{NaYF}_4:18\% \text{Yb}^{3+}/2\% \text{Er}^{3+}$ with phases of hexagonal (white circle: hexagonal- β). (b) TEM images of $\text{NaYF}_4:\text{Yb}^{3+}/\text{Er}^{3+}$. (c) The corresponding distribution of crystallite size of $\text{NaYF}_4:\text{Yb}^{3+}/\text{Er}^{3+}$.

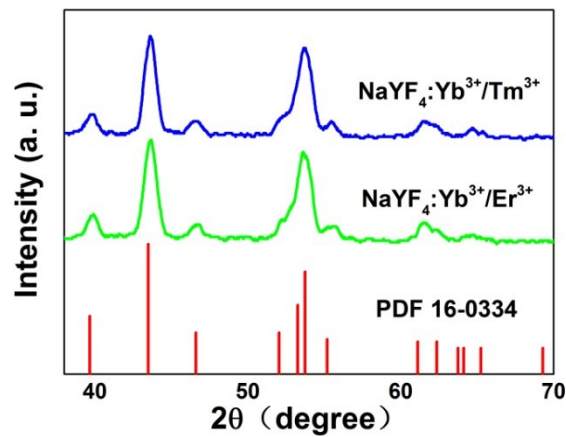


Fig. S3 XRD measurement of $\text{NaYF}_4:18\% \text{Yb}^{3+}/2\% \text{Er}^{3+}$ and $\text{NaYF}_4:18\% \text{Yb}^{3+}/0.5\% \text{Tm}^{3+}$.

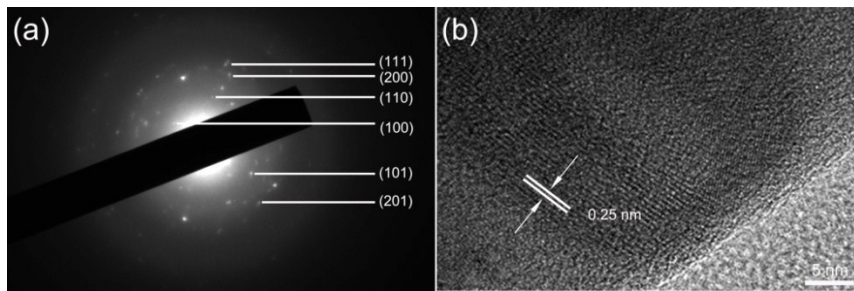


Fig. S4 (a) The representative SAED taken from fabricating microfibers indicating the pure hexagonal phase. (b) HRTEM images of $\text{NaYF}_4:18\%\text{Yb}^{3+}/2\%\text{Er}^{3+}$.

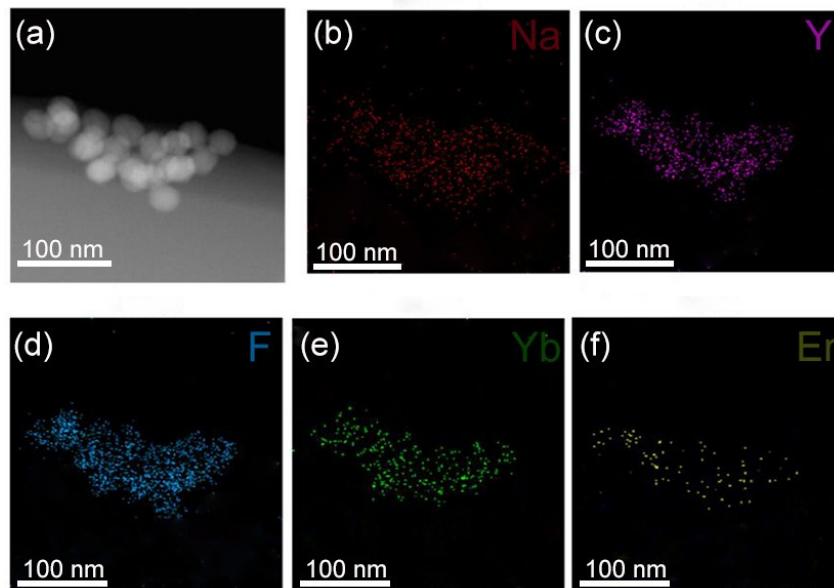


Fig. S5 High-angle annular dark-field (HAADF) images (on the top left) and elemental maps (in other locations) for Na, Y, F, Yb and Er of $\text{NaYF}_4:18\%\text{Yb}^{3+}/2\%\text{Er}^{3+}$.

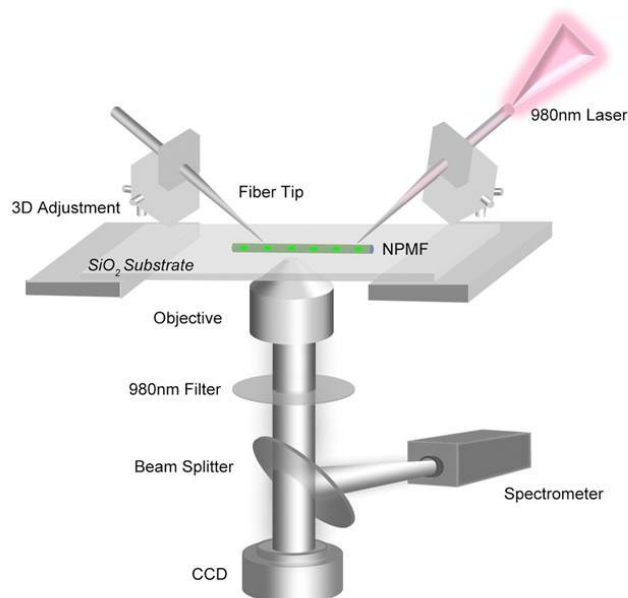


Fig. S6 Schematic of the instrumental setup for the nanoparticle-doped microfiber (NPMF) excitation experiment.

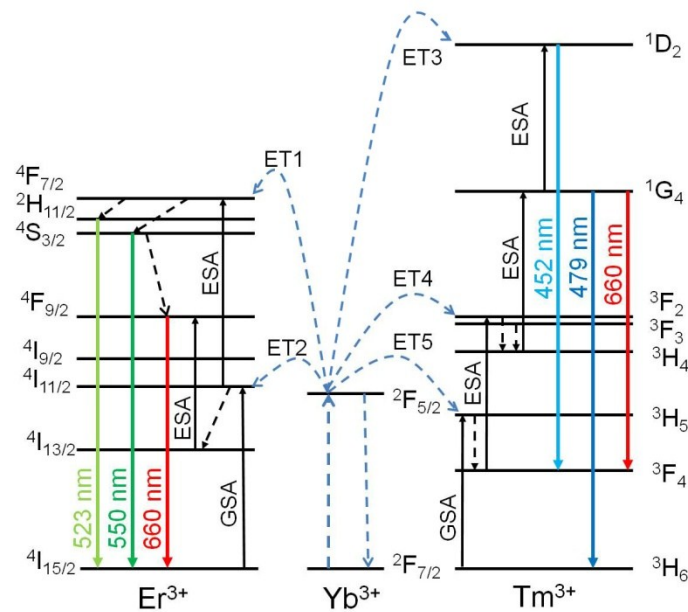


Fig. S7 Energy level diagram of $\text{NaYF}_4:18\%\text{Yb}^{3+}/2\%\text{Er}^{3+}$ and $\text{NaYF}_4:18\%\text{Yb}^{3+}/0.5\%\text{Tm}^{3+}$ and possible up-conversion processes.

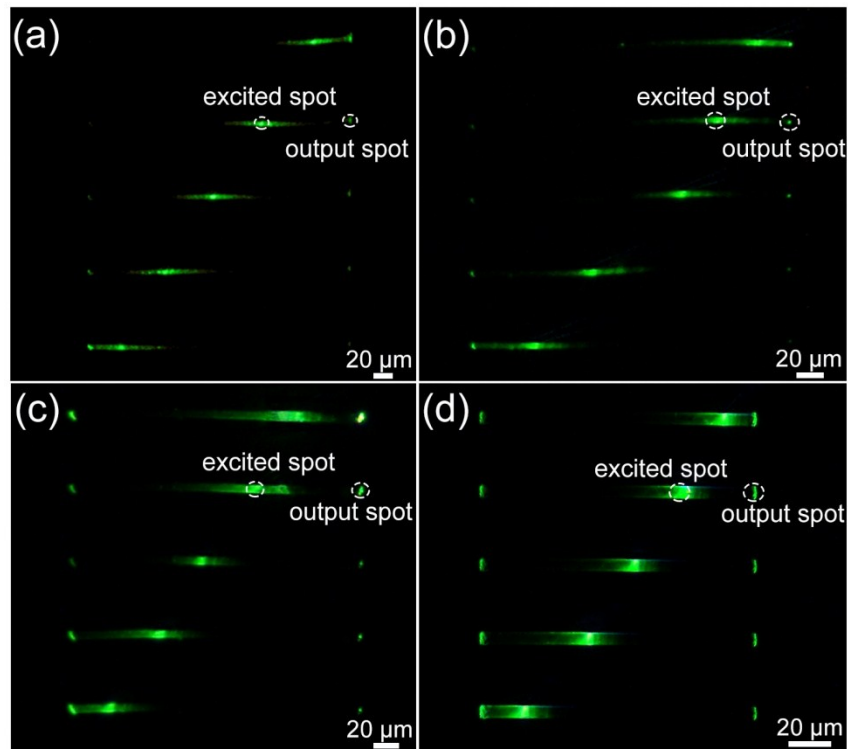


Fig. S8 True-color PL microscope images of $\text{NaYF}_4:18\%\text{Yb}^{3+}/2\%\text{Er}^{3+}/\text{PMMA}$ microfiber was pumped by 980 nm laser with same excitation power. (a) Microfiber with diameter of 2.5 μm . (b) Microfiber with diameter of 4 μm . (c) Microfiber with diameter of 7 μm . (d) Microfiber with diameter of 12 μm .

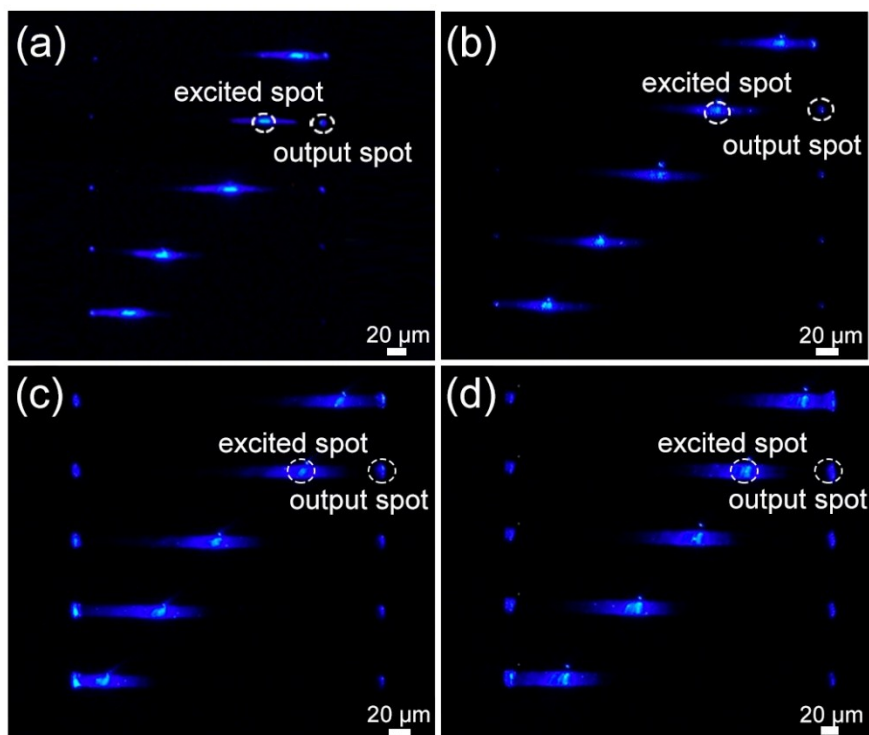


Fig. S9 True-color PL microscope images of $\text{NaYF}_4:18\%\text{Yb}^{3+}/0.5\%\text{Tm}^{3+}/\text{PMMA}$ microfiber was pumped by 980 nm laser with same excitation power. (a) Microfiber with diameter of 2.5 μm . (b) Microfiber with diameter of 5 μm . (c) Microfiber with diameter of 11 μm . (d) Microfiber with diameter of 13.5 μm .

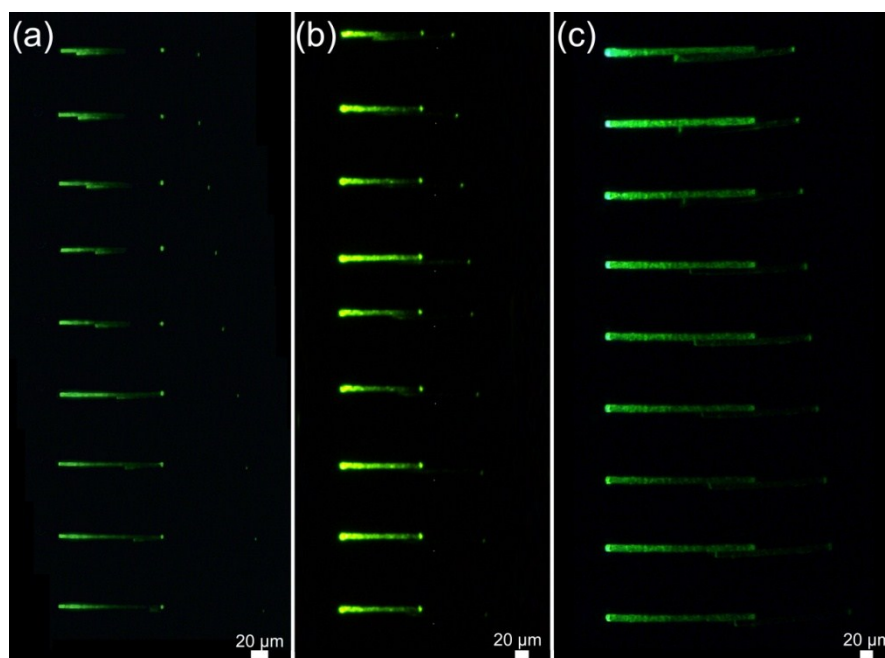


Fig. S10 True color PL micrographs of $\text{NaYF}_4:18\%\text{Yb}^{3+}/2\%\text{Er}^{3+}/\text{PMMA}$ microfibers were pumped with a 980 nm laser at the same excitation power of 0 degrees. (a) Microfiber with diameter of 3 μm . (b) Microfiber with diameter of 7 μm . (c) Microfiber with diameter of 10 μm .

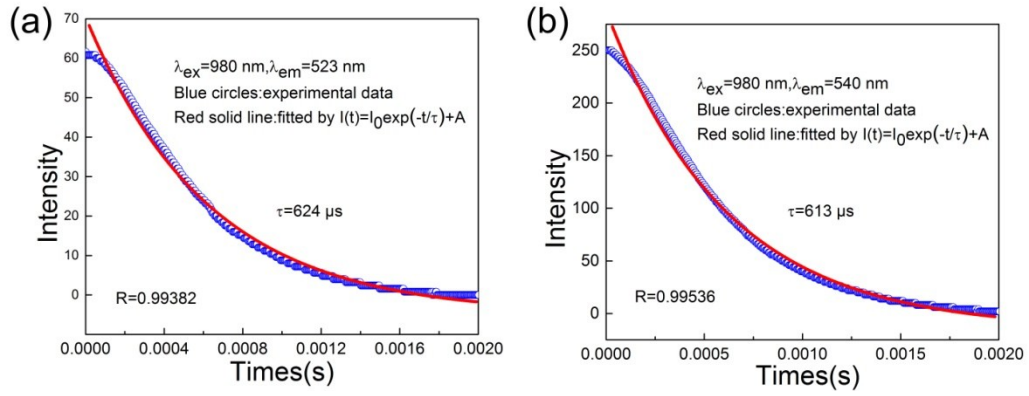


Fig. S11 The decay time of energy transitions of NaYF₄:18%Yb³⁺/2%Er³⁺ NPs. (a) $^2H_{11/2} \rightarrow ^4I_{15/2}$ transition at 523 nm (b) $^4S_{3/2} \rightarrow ^4I_{15/2}$ transition at 540 nm.

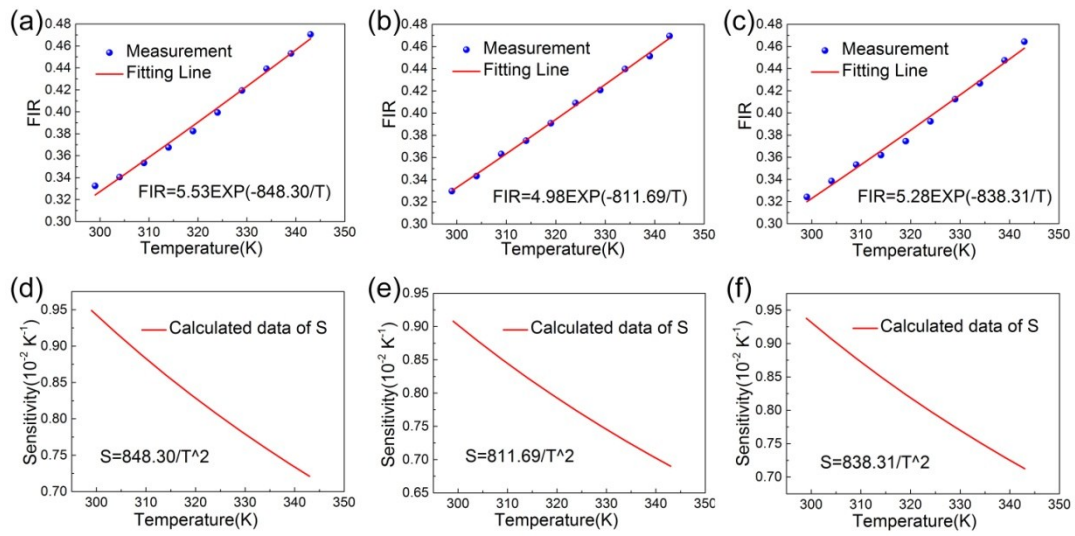


Fig. S12 (a-c) The FIR sensing at the center of three microfibers with a diameter of $\sim 12 \mu m$. (d-f) The corresponding variations of sensitivity versus ambient temperature.

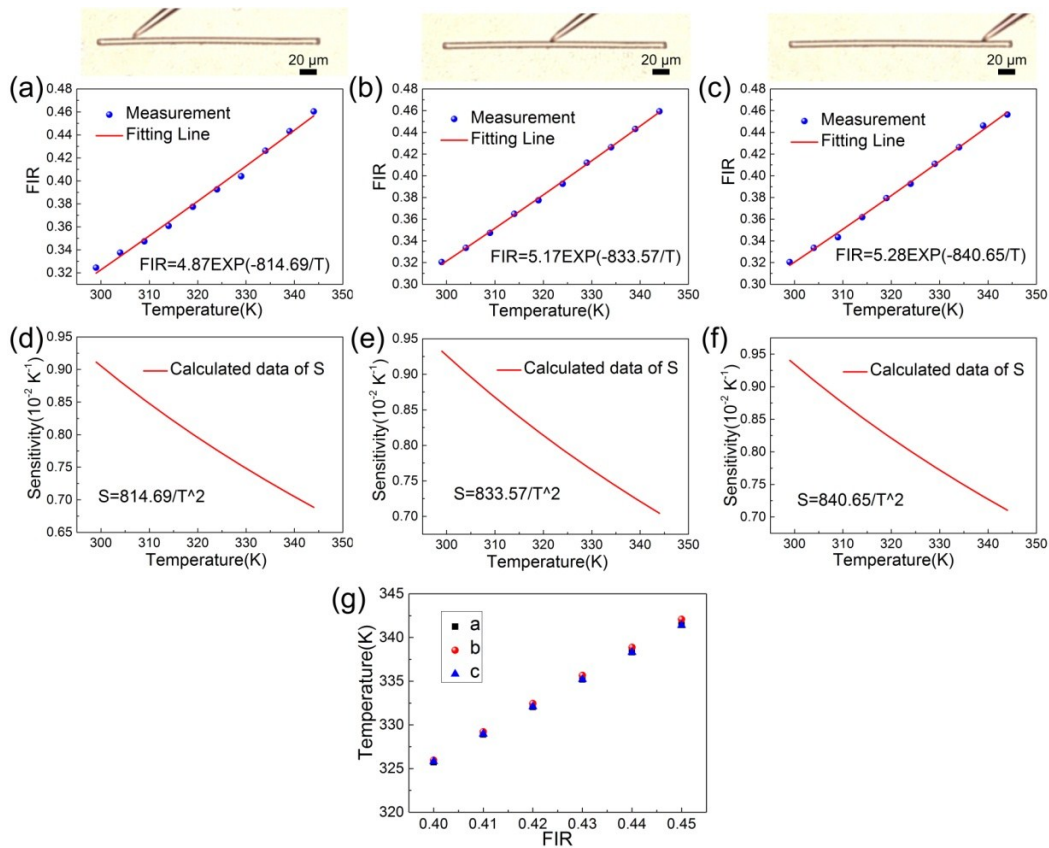


Fig. S13 (a-c) The FIR sensing at the center and both ends of a single fiber with a diameter of 7 μm. (d-f) The corresponding sensitivity at various positions. The bright field images show the specific positions for FIR calibration on a microfiber with length of around 300 μm. (g) The deduced temperatures as a function of FIR values from 0.4 to 0.45, corresponding to the FIR region obtained in the distributed temperature sensing, by using the above three calibration functions.

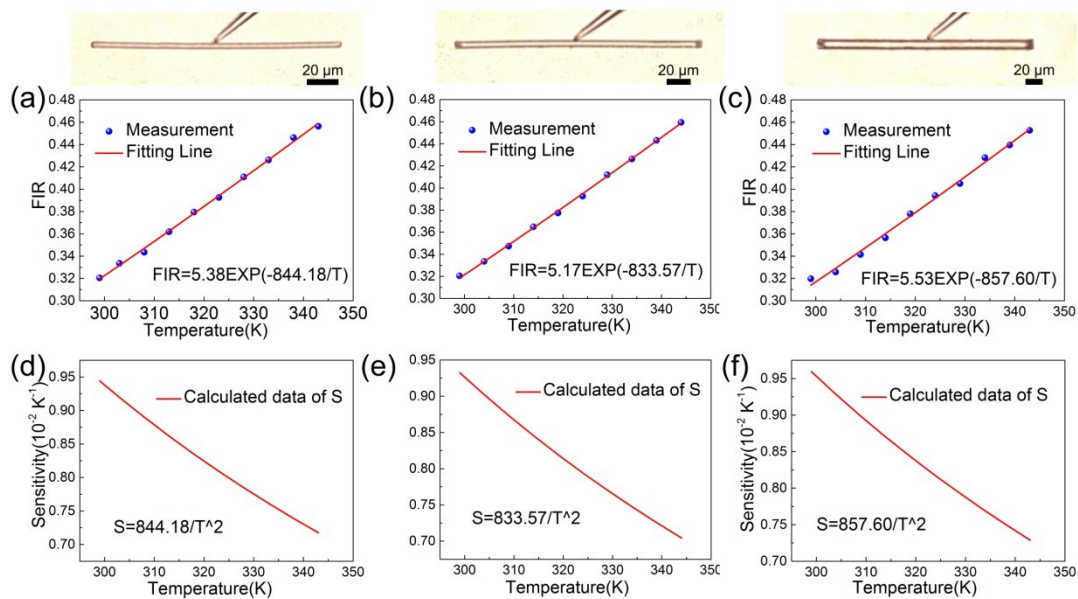


Fig. S14 (a-c) The FIR sensing in the middle of the microfibers with various diameters (4 μm, 7 μm, and 12 μm). (d-f) The corresponding sensitivity of the microfibers with various diameters. The bright field images show the corresponding microfibers with a diameter of 4 μm, 7 μm, and 12 μm.

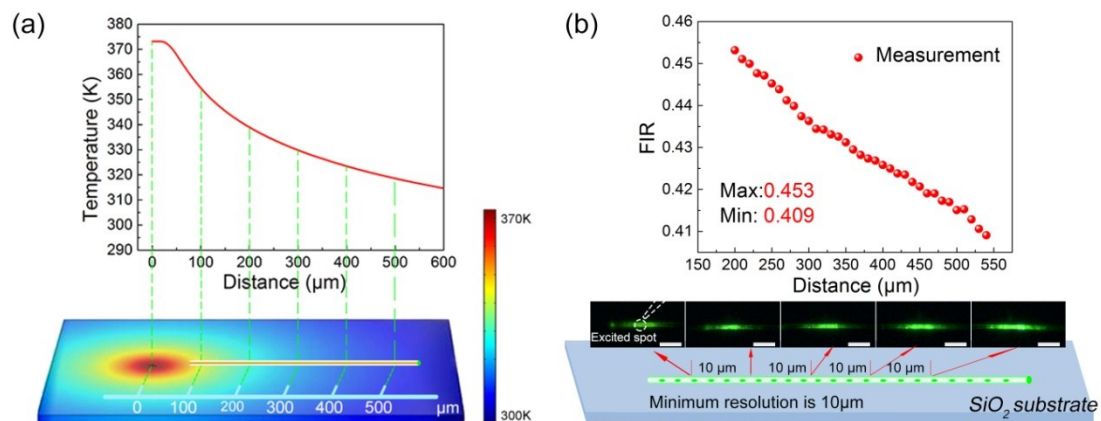


Fig. S15 (a) Photographs of the relationship of temperature and guiding distance (d). The following is the simulation diagram. (b) Photographs of the relationship of actual measured FIR and guiding distance (d). Below is a simple schematic and the inset is microscope image for Er^{3+} -doped microfiber with diameter of 5 μm . The scale bars in the picture are all 20 μm .